Channel Impulse Response-based Source Localization in a Diffusion-based Molecular Communication System

Henry E. Baidoo-Williams*, Muhammad Mahboob Ur Rahman*, Qammer H. Abbasi

***Abstract*—Molecular source localization finds its applications in future healthcare systems, including proactive diagnostics. This work localizes a molecular source in a diffusion based molecular communication (DbMC) system via a minimal set of passive anchor nodes and a fusion center. Two methods are presented which both utilize (the peak of) the channel impulse response measurements to uniquely localize the source, under the assumption that the molecular source of interest lies within the open convex-hull of the sensor/anchor nodes. The first method is a one-shot, triangulation-based approach which estimates the unknown location of the molecular source using least-squares method. The second method is an iterative approach, which utilizes the gradient-descent control law to minimize a non-convex cost function. The corresponding Cramer-Rao bound (CRB) is also derived. Simulation results reveal that: i) the gradient-descent method outperforms the triangulation method (in terms of mean squared error performance) for a wide range of values of signal-to-noise ratio; ii) the gradient-descent method converges to the true source location uniformly (in less than hundred iterations).**

I. Introduction

A nano-scale, molecular communication system consists of a nano-transmitter (emitter) and a nano-receiver (passive, absorbing, ligand-binding) in a fluid medium which are apart by a few micro-meters; information transfer between them is realized via exchange of molecules [1], [2]. In a *diffusion based* molecular communication (DbMC) system, molecules undertake a brownian motion governed by the diffusion process. The very slow diffusion of molecules through the fluid medium implies that the DbMC channel is a low-rate, broadcast channel [3]. DbMC has recently attracted a lot of attention as it helps realize a body-centric network consisting of several (on-body, inside-body) autonomous bionano-machines [1], [2]. Therefore, DbMC has the potential to revolutionize the healthcare system. Additionally, it finds its applications in environmental monitoring and military scenarios [1], [4]. As of today, the researchers have done the noise analysis [5], computed the channel capacity [3], designed modulation schemes [6], optimal receivers [5], and much more (see the survey article [2] which provides a comprehensive overview of the recent development in the field).

Source localization, on the other hand, is the umbrella term for a handful of techniques which locate a signal source by utilizing the measurements collected by a set of sensor/anchor nodes (at known locations). Source localization has been extensively studied to localize a radio-frequency signal source [7], optical source [8], acoustic source [9], and radioactive source [10]. Most of the localization algorithms comprise of the following two steps: i) the sensor nodes construct some measurement (received signal strength, time of arrival, time difference of arrival, pathloss, distance) from the signal received from the signal source of interest, ii) the fusion center fuses the measurements collected by the sensor nodes to minimize an appropriate cost function. To this end, various techniques have been reported in the literature, e.g., semidefinite programming [11],[12], second order cone programming, gradient descent [10], weighted least-squares etc.

Very recently, the researchers have started to investigate the distance estimation methods[1] and the corresponding performance bounds for the DbMC systems [13–17]. In [13], authors estimate the round-trip time and the signal attenuation from the received feedback signal in order to estimate the distance. [14] presents two distance estimation methods based on the peak and energy of the concentration of the received molecules. In [15], Huang et. al. do synchronization-free distance estimation using one-way signaling (via peak concentration and double-spike methods). [16] computes the Cramer-Rao bound (CRB) for distance estimation in a DbMC channel. [17] considers DbMC in a vessel-like environment with passive receivers and Poiseuille flow, and does distance estimation for the two cases of known and unknown emission start time.

Another set of works broadly relevant to the scope of our paper is [18–24] where detection and tracking of a bionano target is performed using self-organizing, mobile bionano-sensors that are capable of releasing attractant and repellent molecules. Specifically, [18] develops a partial differential equations based mathematical model for the target tracking problem. [19] performs target tracking with the aim of targeted drug delivery. [20] carries out in-silico experiments by utilizing chemotactic bacteria and provide some information-theoretic insights on the performance of their proposed target tracking scheme. [21] extends the previous works to track multiple

Henry Ernest Baidoo-Williams is with Amazon, USA.
Muhammad Mahboob Ur Rahman is with the Electrical engineering department, Information Technology University (ITU), Lahore 54000, Pakistan. (mahboob.rahman@itu.edu.pk).
Qammer Hussain Abbasi is with the Department of Electronics and Nano engineering, University of Glasgow, Glasgow, G128qq, UK. (qammer.abbasi@glasgow.ac.uk).
* implies equal contribution by the authors.

[1]Note that a large number of algorithms reported in the literature on localization of a wireless source build upon the distance estimates obtained by the sensor nodes (see [7], [12] and the references therein).

targets. [22, 23] propose a leader-follower model for target tracking, describe the model mathematically and estimate the model parameters via maximum-likelihood approach. Finally, [24] extends [20] by utilizing relay nodes for increased chemotactic efficiency. However, contrary to the works [18–24] which rely solely upon chemical interactions,[2] our work does the localization by leveraging a set of passive, static, sensor nodes which record the measurements and a fusion center that is capable of fusing them to perform the computations.

Contributions and Outlook. This work proposes two novel methods for source localization in a DbMC system, namely, triangulation/least-squares-based method, and gradient descent-based method. For the triangulation-based method, the corresponding CRB is also derived. Some futuristic applications in the healthcare domain that could potentially benefit from this work include early disease (e.g., cancer) detection, targeted drug delivery [19],[26], and quick toxicity detection.

Outline. The rest of this paper is organized as follows. Section II introduces the system model and the DbMC channel model. Section III describes the measurement model used by the two proposed methods. Section IV presents the two proposed methods for source localization. Section V provides some simulation results. Section VI concludes the paper.

II. System Model & Channel Model

A. System Model

Consider a molecular source/emitter, whose location $y^* \in \mathbb{R}^N$ (where $N \in \{2,3\}$) is to be estimated (see Fig. 1). Source localization is done by deploying a set of sensor nodes in close vicinity of the source which report their measurements to a fusion center (FC). The FC is assumed to be a powerful node capable of performing sophisticated signal processing operations (therefore, FC is likely to be an on-body node). As for the sensor nodes, Triangulation based methods have shown that we need at least $n = N+1$ sensors located at $x_i \in \mathbb{R}^N, i \in \{1,\cdots,n\}$ which are non-collinear for $N = 2$ case and non-coplanar for $N = 3$ case. To keep the analysis tractable, this work assumes that: i) the source is a point transmitter, ii) the sensors are passive receivers [27], iii) there is no interference caused by the molecules sent in previous slots, and iv) the reporting channel (i.e., the link between the sensor nodes and the FC) is error-free and delay-free, v) the measurements by the sensor nodes are statistically independent.

Define d_i as the euclidean distance between the source and i-th sensor/anchor node (with known location x_i):

$$d_i = \|x_i - y^*\| \tag{1}$$

where $\|.\|$ is the 2-norm operator.

Next, following assumption is made.

Assumption 2.1: The location of the source node $y^* \in \mathbb{R}^N$ is within the open convex hull of the measurement sensors.

Note that assumption 2.1 can easily be satisfied using coarse initial estimates by perturbing the locations of the measurement sensors.

[2]On a side note, [25] presents two molecular messaging methods (Rosenbrock gradient-ascent algorithm and a chemical encoding messaging method) for localization of a crashed object in a vast underwater search space.

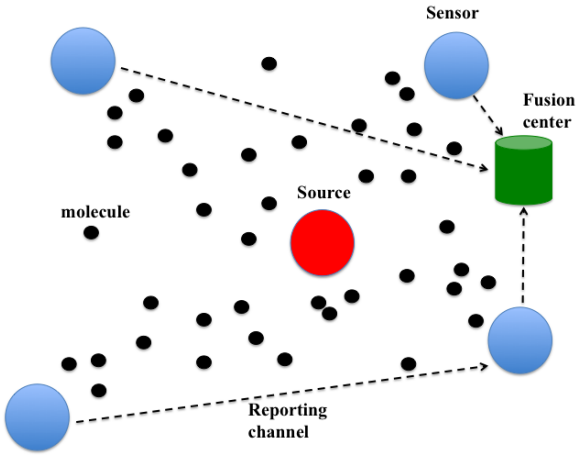

Fig. 1. System model: The molecular source that is to-be localized lies within the convex hull of the nano sensor/anchor nodes (each of which receives the molecules emitted by the source). Moreover, the sensor nodes report their measurements to a fusion center which ultimately does the signal processing to localize the source.

B. The DbMC Channel Model

Consider a DbMC system whereby the transmitter uses pulse-based modulation (i.e., on/off keying) and sends Q molecules within one pulse. Since communication (transport of molecules from source to sensors) takes place through a diffusion paradigm, the DbMC channel can be described as broadcast channel, hence, the transmitter's "message" can be received by all the sensors. Consequently, one can use Fick's second law of diffusion to characterize the mean change in concentration of molecules at a fixed distance d_i w.r.t. time (because diffusion is a stochastic process):

$$\frac{\partial p(d_i,t|d_0)}{\partial t} = D\nabla^2 p(d_i,t|d_0) \tag{2}$$

where ∇^2 is the Laplacian operator, $p(d_i,t|d_0)$ is the molecule distribution function at time t, distance d_i given the initial distance d_0, and D is diffusion coefficient of the medium.

The solution to (2), given in (3), is the expected concentration of molecules as a function of time and distance (which is also the impulse response of the DbMC channel), where $c_i(d_i,t)$ denotes the concentration at distance d_i and time t from the initial transmission time:

$$c_i(d_i,t) = \frac{Q}{(4\pi Dt)^{\frac{N}{2}}} e^{-\frac{d_i^2}{4Dt}} \tag{3}$$

A typical pulse/CIR following the model in (3), as seen by the i-th sensor is shown in Fig. 2.

III. Measurement Model

Assume that L measurements $m_i[l]$ $(l = 1,...,L)$ of channel impulse response (CIR) are taken by sensor i during a single observation interval of length symbol duration:

$$m_i[l] = c_i(d_i,l) + \omega_i[l] = \frac{Q}{(4\pi DlT_s)^{\frac{N}{2}}} e^{-\frac{d_i^2}{4DlT_s}} + \omega_i[l] \tag{4}$$

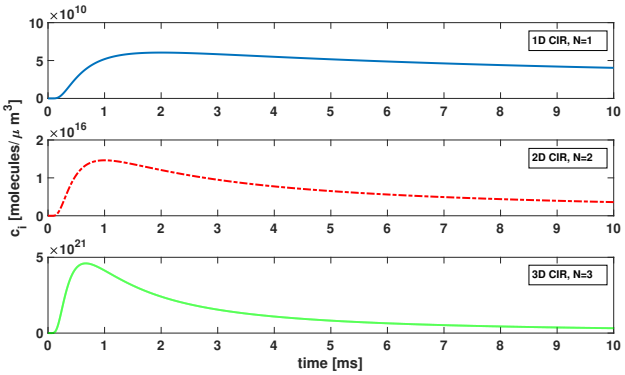

Fig. 2. The received molecular pulse/CIR at i-th sensor that is $d_i = 2$ μm away from the molecular source (for $Q = 5 \times 10^5$, $D = 1e-9$ m^2/sec).

where $\omega_i[l]$ is the Poisson noise, and T_s is the sampling period of the system. In this work, sensor i picks the largest measurement $z_i = \max_l(m_i[l])$ (that corresponds to the instant where received molecular concentration was maximum[3]):

$$z_i = \left(\frac{N}{2\pi}\right)^{\frac{N}{2}} \cdot \left(\frac{1}{e}\right)^{\frac{N}{2}} \cdot \frac{Q}{d_i^N} + \omega_i \tag{5}$$

and sends it to the fusion center.

Definition 3.1: Let $\alpha = \left(\frac{N}{2\pi}\right)^{\frac{N}{2}} \cdot \left(\frac{1}{e}\right)^{\frac{N}{2}} \cdot Q$. Then (5) at sensor i becomes:

$$z_i = \frac{\alpha}{d_i^N} + \omega_i. \tag{6}$$

Assuming that $\omega_i \sim \text{Poisson}(\lambda_i)$ with $\lambda_i = \frac{\alpha}{d_i^N}$, define the signal-to-noise ratio (SNR) γ_i at sensor i as the ratio of the amplitudes of the signal received at sensor i and the noise at sensor i. That is, $\gamma_i = \frac{\alpha/d_i^N}{\sqrt{\alpha/d_i^N}} = \sqrt{\frac{\alpha}{d_i^N}}$. Then, the average SNR at the FC is defined as: $\text{SNR} = \frac{1}{n}\sum_{i=1}^n \gamma_i$.

IV. Source Localization

This section begins with the following assumption:

Assumption 4.1: The location of the sensor $x_i, i \in \{1, \cdots, n\}$ is not coincident with the location of the source, y^*.

Assumption 4.1 makes sense since (5) is undefined otherwise at $x_i = y^*$.

Next, the two proposed methods are presented, one by one.

A. Triangulation-based Localization

The measurements $z_i, i \in \{1, \cdots, n\}$ by the sensors give rise to the following equations:

$$\begin{aligned} z_i = \frac{\alpha}{d_i^N} \Rightarrow \\ \|x_i - y^*\|^N = \frac{\alpha}{z_i} \\ (x_i - y^*)^T(x_i - y^*) = \left(\frac{\alpha}{z_i}\right)^{\frac{2}{N}} \end{aligned} \tag{7}$$

[3]The peak of CIR of the DbMC channel is analogous to the notion of received signal strength in wireless communication.

Taking any two equations from (7), we realise (8).

$$\begin{aligned} x_i^T x_i - x_j^T x_j - 2(x_i^T - x_j^T)y^* = \left(\frac{\alpha}{z_i}\right)^{\frac{2}{N}} - \left(\frac{\alpha}{z_j}\right)^{\frac{2}{N}} \\ -2(x_i^T - x_j^T)y^* = \left(\frac{\alpha}{z_i}\right)^{\frac{2}{N}} - \left(\frac{\alpha}{z_j}\right)^{\frac{2}{N}} - x_i^T x_i + x_j^T x_j \end{aligned} \tag{8}$$

(8) leads to $n_0 = \frac{n(n-1)}{2}$ equations which are used to form the least-squares solution. Define $\mathbf{A} \in \mathbb{R}^{n_0 \times N}$ as:

$$\mathbf{A} = \begin{bmatrix} x_1^T - x_2^T \\ \vdots \\ x_1^T - x_n^T \\ x_2^T - x_3^T \\ \vdots \\ x_{n-1}^T - x_n^T \end{bmatrix} \tag{9}$$

and $\mathbf{B} \in \mathbb{R}^{n_0 \times 1}$ as:

$$\mathbf{B} = \begin{bmatrix} \left(\frac{\alpha}{z_1}\right)^{\frac{2}{N}} - \left(\frac{\alpha}{z_2}\right)^{\frac{2}{N}} - x_1^T x_1 + x_2^T x_2 \\ \vdots \\ \left(\frac{\alpha}{z_1}\right)^{\frac{2}{N}} - \left(\frac{\alpha}{z_n}\right)^{\frac{2}{N}} - x_1^T x_1 + x_n^T x_n \\ \left(\frac{\alpha}{z_2}\right)^{\frac{2}{N}} - \left(\frac{\alpha}{z_3}\right)^{\frac{2}{N}} - x_2^T x_2 + x_3^T x_3 \\ \vdots \\ \left(\frac{\alpha}{z_{n-1}}\right)^{\frac{2}{N}} - \left(\frac{\alpha}{z_n}\right)^{\frac{2}{N}} - x_{n-1}^T x_{n-1} + x_n^T x_n \end{bmatrix} \tag{10}$$

Then, the triangulation-based estimate $\hat{y}$ of location of the molecular source is given by:

$$\hat{y} = \left(\mathbf{A}^T\mathbf{A}\right)^{-1}\mathbf{A}^T\mathbf{B} \tag{11}$$

B. Gradient-Descent Localization

Lemma 4.1: Under (5) and assumption 4.1, z_i is analytic and a strictly decreasing function of d_i in the noise-free case.

Proof: Notice that

$$\dot{z_i} = -N\frac{\alpha}{d_i^{N+1}} \leq 0 \quad \forall i \tag{12}$$

This concludes the proof. ■

Consequent to Lemma 4.1, one could apply the gradient-descent minimization procedure to the following non-convex cost function [10]:

$$J(y) = \sum_{i=1}^n (z_i - g(d_i))^2 \tag{13}$$

where $g(d_i) = \frac{\alpha}{d_i^N}$. Then, the gradient-descent control law at fusion center is the following:

$$y[k+1] = y[k] - \mu \frac{\partial J(y)}{\partial y}\bigg|_{y=y[k]} \tag{14}$$

where $\mu > 0$ is the step size, and k is the iteration number of the algorithm. With the knowledge of Q, D, z_i and $y[k]$, (14) is implementable at the fusion center. Specifically, the gradient of y is given as:

$$\frac{\partial J(y)}{\partial y} = 2\sum_{i=1}^n \frac{(z_i - g_i(d_i))\dot{g}_i(d_i)(y - x_i)}{d_i} \tag{15}$$

It has been shown in [10] that given (15), suppose there are precisely $n = N + 1$ measurement sensors in $\mathbb{R}^N$, and the source y^* is in the open convex hull of the sensor locations $x_i, i \in \{1, \cdots, N+1\}$, then: (i) there is a unique point within the open convex hull of the sensor locations where (15) and (13) are identically zero, (ii) the gradient-descent law converges uniformly to the true optima, i.e., $y*$ in the absence of noise. Notice that this is the same minimum number of sensors required for triangulation-based methods.

C. Cramer-Rao Bound Analysis

Finally, the Cramer-Rao bound (CRB) for the measurement model of (6) is computed. Due to statistically independent measurements by the sensor nodes, the fusion center constructs the joint probability density function as follows:

$$f_{(y^*|z_1,\cdots,z_n)} = \prod_{i=1}^{n} \frac{\left(\frac{\alpha}{d_i^N}\right)^{z_i} e^{-\frac{\alpha}{d_i^N}}}{z_i!} \tag{16}$$

The log-likelihood function, $\log f_{(y^*|z_1,\cdots,z_n)} = L_{(y^*|z_1,\cdots,z_n)}$ is:

$$\begin{aligned} L_{(y^*|z_1,\cdots,z_n)} &= \sum_{i=1}^{n} z_i \log \frac{\alpha}{d_i^N} - \frac{\alpha}{d_i^N} - \log z_i! \\ &= -\left(\sum_{i=1}^{n} N z_i \log d_i + \frac{\alpha}{d_i^N}\right) + \kappa_{(z_1,\cdots,z_n)} \end{aligned} \tag{17}$$

where $\kappa_{(z_1,\cdots,z_n)}$ is a constant. The first and second derivatives with respect to y^* will yield:

$$\dot{L}_{(y^*|z_1,\cdots,z_n)} = N \sum_{i=1}^{n} \left(\frac{\alpha}{d_i^{N+1}} - \frac{z_i}{d_i}\right) \frac{1}{d_i} (y^* - x_i) \tag{18}$$

$$\begin{aligned} \ddot{L}_{(y^*|z_1,\cdots,z_n)} = -N \Bigg[&\sum_{i=1}^{n} \left(\frac{\alpha(N+2)}{d_i^{N+4}} - \frac{2z_i}{d_i^4}\right) (y^* - x_i)(y^* - x_i)^T \\ &+ \left(\frac{z_i}{d_i^2} - \frac{\alpha}{d_i^{N+2}}\right) \mathbf{I}_{n\times n} \Bigg] \end{aligned} \tag{19}$$

where $\mathbf{I}_{n\times n}$ is the identity matrix of size $n \times n$. From (19), one could compute the Fisher information matrix (FIM) as:

$$-\mathrm{E}\left[\ddot{L}_{(y^*|z_1,\cdots,z_n)}\right] = N^2 \alpha \sum_{i=1}^{n} \frac{(y^* - x_i)(y^* - x_i)^T}{d_i^{N+4}} \tag{20}$$

where $\mathrm{E}(.)$ is the expectation operator. The CRB is thus the trace of the inverse of (20):

$$\mathrm{CRB} = \mathrm{Tr}\left[\left(N^2 \alpha \sum_{i=1}^{n} \frac{(y^* - x_i)(y^* - x_i)^T}{d_i^{N+4}}\right)^{-1}\right] \tag{21}$$

where $\mathrm{Tr}(.)$ is the trace of a matrix.

V. Numerical Results

Simulations were performed for $N = 2, n = 3$, and $Q = 50$. Fig. 3 (a) investigates the mean squared error (MSE) performance of the triangulation method and the gradient-descent method (as well as the CRB) against the average SNR at the FC. To generate Fig. 3 (a), Monte-Carlo simulations were performed with 5000 realizations of z_i, while the MSE of the gradient-descent method was recorded after 100 iterations (for each SNR value). Fig. 3 (a) shows that the CRB and the MSE of both methods decrease with the increase in the SNR, as expected. Moreover, the curve for the gradient-descent method is nearly super-imposed onto the CRB curve. Thus, gradient-descent method outperforms the triangulation method for the whole range of interest of the SNR values (of course, at the cost of increased complexity due to iterative nature of the gradient-descent method). Fig. 3 (b) plots the squared error $\|\hat{y} - y^*\|^2$ against the number of iterations k. Note that the error vanishes uniformly, i.e., the gradient descent-based method converges to the true optima/source location in less than hundred iterations.

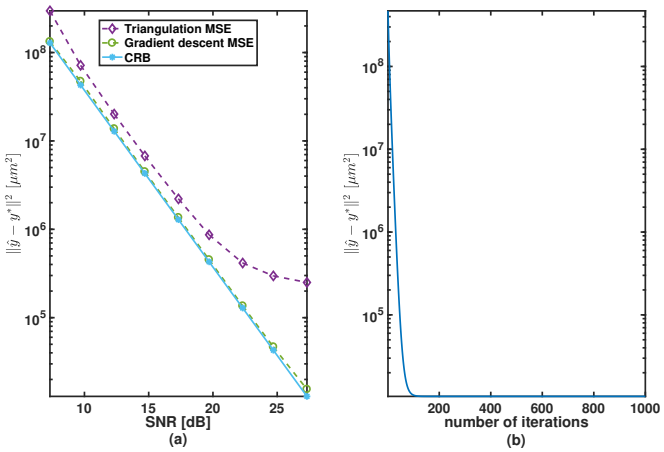

Fig. 3. (a) Gradient-descent method outperforms the triangulation method for whole range of interest of SNR values, (b) the squared error of the gradient-descent method decreases monotonically with number of iterations k.

Fig. 4 (a) & (b) show a 2D layout to demonstrate the localization performance of the triangulation method and gradient-descent method, respectively. For this plot, the molecular source was placed within the convex hull of the three sensor nodes. Fig. 4 (a) shows that the triangulation-based location estimate given by (11) is quite close to the true source location. Fig. 4 (b) shows that the trajectory of the iterated estimates $y[k]$ of the gradient-descent method converges to the true source location quickly (in less than hundred iterations).

VI. Conclusion

This work presented two methods which both utilized (the peak of) the channel impulse response measurements to uniquely localize a molecule emitter. The first method, the triangulation-based approach, estimated the unknown location of the molecular source using the least-squares method. The second method utilized the gradient-descent control law to

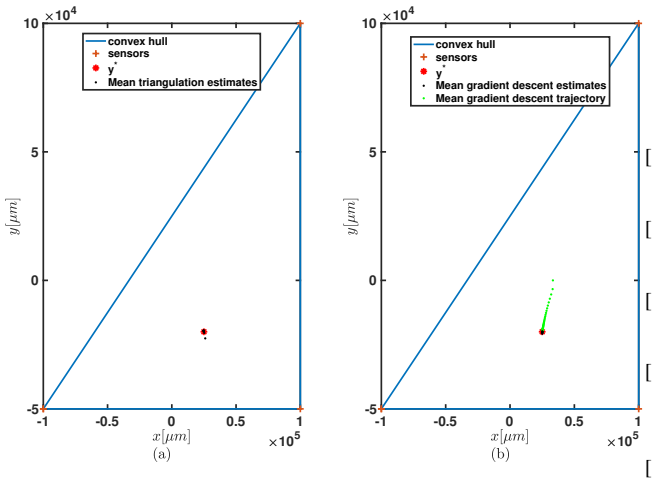

Fig. 4. Consider a 2D layout with the source lying within the convex hull of the $n = 3$ sensors. (a) the location estimate provided by the triangulation method is quite close to the true source location, (b) the iterates of the location estimate provided by the gradient-descent method converge to the true source location uniformly.

minimize a non-convex cost function. The corresponding CRB was also derived. Simulation results revealed that the gradient-descent method outperforms the triangulation method (in terms of the MSE performance) for the whole range of interest of the SNR values.

Some futuristic applications in the healthcare domain that could potentially benefit from the proposed method include early disease detection, targeted drug delivery, and quick toxicity detection.

One potential follow-up work could be to do source localization using time-of-arrival measurements and compare its performance against the two CIR-based localization methods proposed in this work. Another promising direction will be to consider the effect of interference caused by previously sent molecules on the performance of the proposed source localization methods.

REFERENCES

[1] T. Nakano, "Molecular communication: A 10 year retrospective," *IEEE Transactions on Molecular, Biological and Multi-Scale Communications*, vol. 3, no. 2, pp. 71–78, June 2017.

[2] J. Wang, B. Yin, and M. Peng, "Diffusion based molecular communication: principle, key technologies, and challenges," *China Communications*, vol. 14, no. 2, pp. 1–18, February 2017.

[3] M. Pierobon and I. F. Akyildiz, "Capacity of a diffusion-based molecular communication system with channel memory and molecular noise," *IEEE Transactions on Information Theory*, vol. 59, no. 2, pp. 942–954, Feb 2013.

[4] I. F. Akyildiz, F. Brunetti, and C. Blazquez, "Nanonetworks: A new communication paradigm," *Computer Networks*, vol. 52, no. 12, pp. 2260 – 2279, 2008. [Online]. Available: http://www.sciencedirect.com/science/article/pii/S1389128608001151

[5] I. Llatser, A. Cabellos-Aparicio, M. Pierobon, and E. Alarcon, "Detection techniques for diffusion-based molecular communication," *IEEE Journal on Selected Areas in Communications*, vol. 31, no. 12, pp. 726–734, December 2013.

[6] M. S. Kuran, H. B. Yilmaz, T. Tugcu, and I. F. Akyildiz, "Modulation techniques for communication via diffusion in nanonetworks," in *IEEE International Conference on Communications (ICC)*, 2011, pp. 1–5.

[7] A. Sayed, A. Tarighat, and N. Khajehnouri, "Network-based wireless location: challenges faced in developing techniques for accurate wireless location information," *IEEE Signal Processing Magazine*, vol. 22, no. 4, pp. 24–40, July 2005.

[8] J. Armstrong, Y. A. Sekercioglu, and A. Neild, "Visible light positioning: a roadmap for international standardization," *IEEE Communications Magazine*, vol. 51, no. 12, pp. 68–73, December 2013.

[9] T. Kundu, "Acoustic source localization," *Ultrasonics*, vol. 54, no. 1, pp. 25 – 38, 2014. [Online]. Available: http://www.sciencedirect.com/science/article/pii/S0041624X13001819

[10] H. Baidoo-Williams, S. Dasgupta, R. Mudumbai, and E. Bai, "On the gradient descent localization of radioactive sources," *IEEE Signal Processing Letters*, vol. 20, no. 11, pp. 1046–1049, Nov 2013.

[11] C. Meng, Z. Ding, and S. Dasgupta, "A semidefinite programming approach to source localization in wireless sensor networks," *IEEE Signal Processing Letters*, vol. 15, pp. 253–256, 2008.

[12] E. Xu, Z. Ding, and S. Dasgupta, "Source localization in wireless sensor networks from signal time-of-arrival measurements," *IEEE Transactions on Signal Processing*, vol. 59, no. 6, pp. 2887–2897, June 2011.

[13] M. Moore, T. Nakano, A. Enomoto, and T. Suda, "Measuring distance from single spike feedback signals in molecular communication," *IEEE Transactions on Signal Processing*, vol. 60, no. 7, pp. 3576–3587, July 2012.

[14] X. Wang, M. D. Higgins, and M. S. Leeson, "Distance estimation schemes for diffusion based molecular communication systems," *IEEE Communications Letters*, vol. 19, no. 3, pp. 399–402, March 2015.

[15] J.-T. Huang, H.-Y. Lai, Y. Lee, C. Lee, and P. Yeh, "Distance estimation in concentration-based molecular communications," in *IEEE Global Communications Conference (GLOBECOM)*, Dec 2013, pp. 2587–2591.

[16] A. Noel, K. C. Cheung, and R. Schober, "Bounds on distance estimation via diffusive molecular communication," in *IEEE Global Communications Conference (GLOBECOM)*, Dec 2014, pp. 2813–2819.

[17] M. Turan, B. C. Akdeniz, M. Å. Kuran, H. B. Yilmaz, I. Demirkol, A. E. Pusane, and T. Tugcu, "Transmitter localization in vessel-like diffusive channels using ring-shaped molecular receivers," *IEEE Communications Letters*, vol. 22, no. 12, pp. 2511–2514, Dec 2018.

[18] Y. Okaie, T. Nakano, T. Hara, K. Hosoda, Y. Hiraoka, and S. Nishio, "Modeling and performance evaluation of mobile bionanosensor networks for target tracking," in *IEEE International Conference on Communications (ICC)*, June 2014, pp. 3969–3974.

[19] Y. Okaie, T. Nakano, T. Hara, T. Obuchi, K. Hosoda, Y. Hiraoka, and S. Nishio, "Cooperative target tracking by a mobile bionanosensor network," *IEEE Transactions on NanoBioscience*, vol. 13, no. 3, pp. 267–277, Sep. 2014.

[20] Y. Okaie, T. Obuchi, T. Hara, and S. Nishio, "In silico experiments of mobile bionanosensor networks for target tracking," in *Proceedings of the Second Annual International Conference on Nanoscale Computing and Communication*. ACM, 2015, p. 14.

[21] S. Iwasaki, J. Yang, A. O. Abraham, J. L. Hagad, T. Obuchi, and T. Nakano, "Modeling multi-target detection and gravitation by intelligent self-organizing bioparticles," in *IEEE Global Communications Conference (GLOBECOM)*, Dec 2016, pp. 1–6.

[22] a. Nakano, a. Kobayashi, a. Koujin, a. Chen-Hao Chan, a. Yu-Hsiang Hsu, a. Okaie, a. Obuchi, a. Hara, a. Hiraoka, and a. Haraguchi, "Leader-follower based target detection model for mobile molecular communication networks," in *IEEE 17th International Workshop on Signal Processing Advances in Wireless Communications (SPAWC)*, July 2016, pp. 1–5.

[23] T. Nakano, Y. Okaie, S. Kobayashi, T. Koujin, C. Chan, Y. Hsu, T. Obuchi, T. Hara, Y. Hiraoka, and T. Haraguchi, "Performance evaluation of leaderâfollower-based mobile molecular communication networks for target detection applications," *IEEE Transactions on Communications*, vol. 65, no. 2, pp. 663–676, Feb 2017.

[24] L. Yang, Y. Mao, Q. Liu, H. Zhai, and K. Yang, "High-efficiency target detection scheme through relay nodes in chemotactic-based molecular communication," in *IEEE International Conference on Sensing, Communication and Networking (SECON Workshops)*, June 2018, pp. 1–4.

[25] S. Qiu, W. Guo, B. Li, Y. Wu, X. Chu, S. Wang, and Y. Y. Dong, "Long range and long duration underwater localization using molecular messaging," *IEEE Transactions on Molecular, Biological and Multi-Scale Communications*, vol. 1, no. 4, pp. 363–370, Dec 2015.

[26] N. R. Raz, M. Akbarzadeh-T.*, and M. Tafaghodi, "Bioinspired nanonetworks for targeted cancer drug delivery," *IEEE Transactions on NanoBioscience*, vol. 14, no. 8, pp. 894–906, Dec 2015.

[27] A. Noel, Y. Deng, D. Makrakis, and A. Hafid, "Active versus passive: Receiver model transforms for diffusive molecular communication," in *IEEE Global Communications Conference (GLOBECOM)*, 2016, pp. 1–6.